Angewandte Chemie

DOI: 10.1002/anie.200700304

Hydride Generation

Photochemical and Radiolytic Production of an Organic Hydride Donor with a Ru^{II} Complex Containing an NAD^+ Model Ligand**

Dmitry Polyansky, Diane Cabelli, James T. Muckerman, Etsuko Fujita, Take-aki Koizumi, Takashi Fukushima, Tohru Wada, and Koji Tanaka**

Nicotinamide adenine dinucleotide (NAD^+) is one of the most important redox mediators in biological systems and acts as a reservoir/source of two electrons and a proton.[1] The NAD^+/NADH redox couple has been drawing much attention because bioinspired chemical reactions that produce neither high-energy intermediates nor unwanted by-products promise to be key factors in realizing sustainable energy sources. Large numbers of photochemical reactions mediated by NADH model compounds, such as reduction of alkyl halides, olefins, and ketones and photoinduced electron transfer, as well as thermal reactions using NADH analogues, have been extensively studied.[2] However, all the reactions mediated with NADH models are limited to stoichiometric reactions. We recently prepared a polypyridylruthenium complex with an NAD^+/NADH model ligand, $[Ru(bpy)_2(pbn)]^{2+}$ ($[\mathbf{1}]^{2+}$; bpy = 2,2′-bipyridine, pbn = 2-(2-pyridyl)benzo[*b*]-1,5-naphthyridine), which acts as a catalyst in the electrochemical reduction of acetone to 2-propanol, similar to the enzymatic NAD^+/NADH.[3] While the mechanism remains unclear, this is the first example indicating that an NADH model complex such as $[Ru(bpy)_2(pbnHH)]^{2+}$ ($[(\mathbf{1})HH]^{2+}$, or other intermediates in this system) works as a catalytic hydride donor for the formation of 2-propanol. Herein, we report clear evidence of the photochemical and radiolytic formation of $[(\mathbf{1})HH]^{2+}$ with H^+. The results open a new door for photocatalytic hydride (or proton-coupled electron) transfer reactions originating from metal-to-ligand charge-transfer (MLCT) excited states of metal complexes with a bioinspired NADH-like ligand.

First, we examined the acid–base and electrochemical properties of the ground and excited states of $[\mathbf{1}]^{2+}$. The titration of an aqueous solution containing $[\mathbf{1}]^{2+}$ with acid shows the disappearance of $[\mathbf{1}]^{2+}$ (λ_{max} = 355, 375, 390 sh, 430, and 533 nm) and the appearance of $[H(\mathbf{1})]^{3+}$ (λ_{max} = 378 and 610 nm), with a pK_a of 1.7 for $[H(\mathbf{1})]^{3+}$ (Figure 1). The cyclic voltammogram of $[\mathbf{1}]^{2+}$ in CH_3CN shows reversible waves at 0.66, −0.72, −1.34, and −1.62 V versus SCE, which can be assigned to Ru^{2+}/Ru^{3+}, $pbn^{\bullet-}$/pbn, (bpy, $bpy^{\bullet-}$)/$(bpy)_2$, and $(bpy^{\bullet-})_2$/(bpy, $bpy^{\bullet-}$), respectively. However, the potential for $pbn^{\bullet-}$/pbn is pH dependent (59 mV/pH) between pH 2 and 11 in H_2O (Figure 2). This finding indicates that the one-electron reduction is coupled with a proton-transfer reaction to form the neutral ligand radical $[Ru(bpy)_2(pbnH^{\bullet})]^{2+}$.

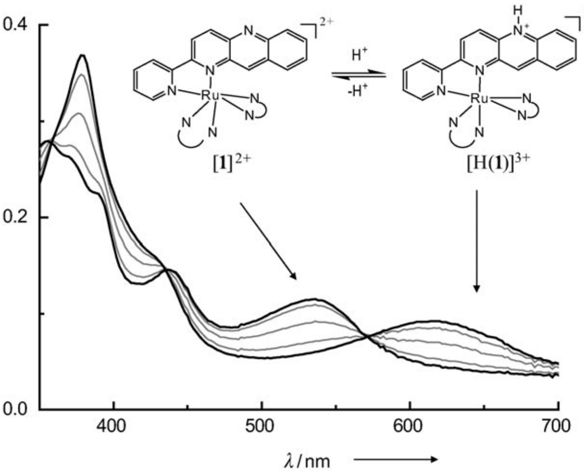

Figure 1. pH-dependent UV/Vis spectra of $[\mathbf{1}]^{2+}$ (1.5×10^{-5} M) in H_2O.

TD-B3LYP/LANL2DZ calculations of $[\mathbf{1}]^{2+}$ in both the gas phase and in a self-consistent-reaction-field, polarizable continuum model of acetonitrile yielded the spectra shown in Figure S1 in the Supporting Information. The two strong lines in the solution-phase spectrum at 510 and 429 nm correspond to HOMO−1 to LUMO and HOMO−2 to LUMO+1 transitions, respectively (Figure 3 and Figure S2 in the Supporting Information). The positions and intensities of the gas-phase transitions between 500 and 450 nm are significantly affected by solvation. The solution-phase spectrum is in better accord with the experimental spectrum shown in Figure 4. B3LYP/LANL2DZ calculations show that the HOMO is primarily a Ru d orbital and the LUMO is almost exclusively

---

[*] Dr. D. Polyansky, Dr. D. Cabelli, Dr. J. T. Muckerman, Dr. E. Fujita
Chemistry Department
Brookhaven National Laboratory
Upton, NY 11973-5000 (USA)
Fax: (+1) 631-344-4356
E-mail: fujita@bnl.gov
Homepage: http://www.chemistry.bnl.gov/SciandTech/PRC/fujita/fujita.html

Dr. T. Koizumi, T. Fukushima, Dr. T. Wada, Prof. K. Tanaka
Coordination Chemistry Laboratories
Institute for Molecular Science and CREST
Japan Science and Technology Agency
5-1 Higashiyama, Myodaiji, Okazaki, Aichi 444-8787 (Japan)
Fax: (+81) 564-59-5582
E-mail: ktanaka@ims.ac.jp

[**] Work performed at Brookhaven National Laboratory was funded under contract DE-AC02-98CH10886 with the U.S. Department of Energy and supported by its Division of Chemical Sciences, Geosciences, and Biosciences, Office of Basic Energy Sciences. NAD^+ = nicotinamide adenine dinucleotide.

Supporting information for this article is available on the WWW under http://www.angewandte.org or from the author.

a delocalized pbn π* orbital (Figure 3). The HOMO−1 and (especially) the HOMO−2 have a large Ru d orbital composition, while the LUMO + 1 is a π* orbital delocalized over the two bpy ligands. The two strong transitions in the solution-phase spectrum thus have a MLCT character. The experimental spectra for the formation of $[H(\mathbf{1})]^{3+}$ (Figure 1), based on pbn undergoing a red shift of the 533-nm band upon protonation, agree with this result.

The excited-state spectrum of $[\mathbf{1}]^{2+}$ in CH_3CN upon 355-nm laser excitation is shown in Figure S3 B in the Supporting Information. The lifetime of $*[\mathbf{1}]^{2+}$ is 140 and ≈40 ns in CH_3CN and H_2O (pH 6), respectively. The excited state decays rapidly below pH 2.0, which indicates that the lifetime of the excited state of $[H(\mathbf{1})]^{3+}$ ($*[H(\mathbf{1})]^{3+}$) is short (< 10 ns). The protonation of $*[\mathbf{1}]^{2+}$ is fast, but the deprotonation of $*[H(\mathbf{1})]^{3+}$ is slow. Therefore an equilibrium between the protonated and nonprotonated excited states is not reached.

The excited state of $[\mathbf{1}]^{2+}$ was reductively quenched by an amine to produce the one-electron-reduced species in dry organic solvents. The spectrum obtained using 1,4-diazabicyclo[2.2.2]octane (DABCO) is shown in Figure S3 C in the Supporting Information; it is consistent with that obtained by Na–Hg reduction in CH_3CN (Figure S3 A in the Supporting Information) except for an additional broad absorption band that results from the formation of the DABCO radical cation. The one-electron-reduced species is a pbn ligand radical anion and is stable in CH_3CN. However, continuous photolysis ($\lambda > 300$ nm) of a CH_3CN/Et_3N or dimethylformamide/triethanolamine (DMF/TEOA) solution (4:1, v/v) containing $[\mathbf{1}](PF_6)_2$ causes a decrease in the absorption bands of $[\mathbf{1}]^{2+}$ ($\lambda_{max} = 355$, 375, 430, and 533 nm) and the appearance of a new species with bands ($\lambda_{max} =$ 417 nm with a shoulder at ca. 460 nm) as shown in Figure 4, without indicating the formation of the one-electron-reduced species presented above. A similar spectral change was obtained upon irradiation at (580 ± 6) nm. The high-resolution electrospray ionization (HR-ESI) mass spectrum (Figure S4 in the Supporting Information) of the final solution displayed a parent peak at m/z 366.5725 ($z = 2$), consistent with the formation of $[(\mathbf{1})HH]^{2+}$ by the reaction of two protons and two photoproduced electrons as found in the biological NAD^+/NADH system. The quantum yield for the formation of $[(\mathbf{1})HH]^{2+}$ is 0.21 at $\lambda = (355 \pm 6)$ nm.

To further understand the properties of $[(\mathbf{1})HH]^{2+}$, we prepared $[(\mathbf{1})HH]^{2+}$ in high yield by treatment of $[\mathbf{1}](PF_6)_2$ with two equivalents of $Na_2S_2O_4$ in CH_3CN/H_2O (1:1, v/v). The spectral change associated with the reaction is similar to that shown in Figure 4. Single crystals of $[(\mathbf{1})HH](PF_6)_2{\cdot}2\,CH_3CN$ suitable for an X-ray diffraction study were obtained by recrystallization from acetonitrile with vapor diffusion of ethyl ether.[4] The molecular structure of $[(\mathbf{1})HH]^{2+}$ (Figure 5) is very close to that of $[\mathbf{1}]^{2+}$[3] except for the pbn and $pbnH_2$ ligands. Elongation of the C8−C10 and C8−C12 bonds of $[(\mathbf{1})HH]^{2+}$ (1.510(4) and 1.498(6) Å)

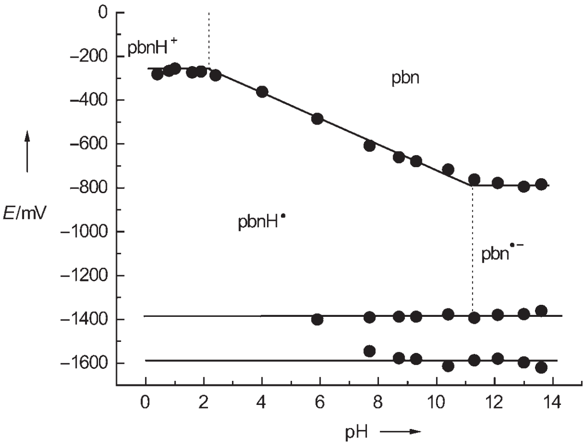

Figure 2. pH-dependent reduction potentials of $[\mathbf{1}]^{2+}$ in H_2O with 5 mM phosphate buffer between pH 3 and 10. The two lines below −1400 mV indicate the reduction of bpy.

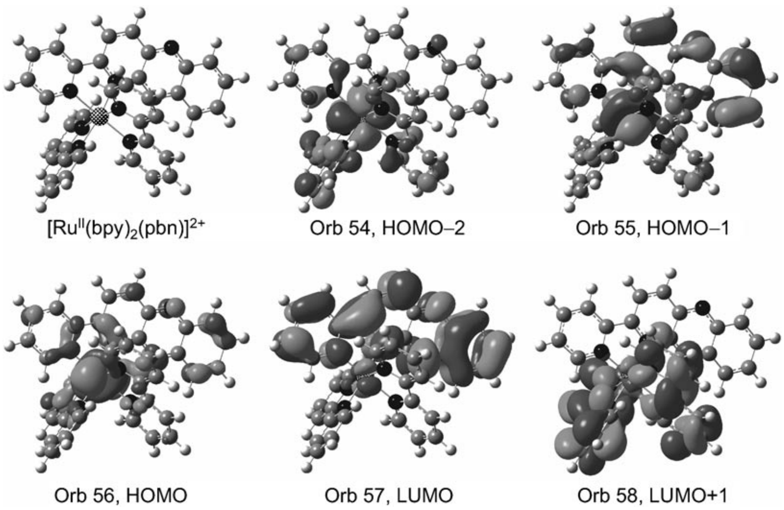

Figure 3. Optimized structure and frontier orbitals from a B3LYP/LANL2DZ calculation of $[Ru^{II}(bpy)_2(pbn)]^{2+}$ in a self-consistent-reaction-field, polarizable continuum model of acetonitrile.

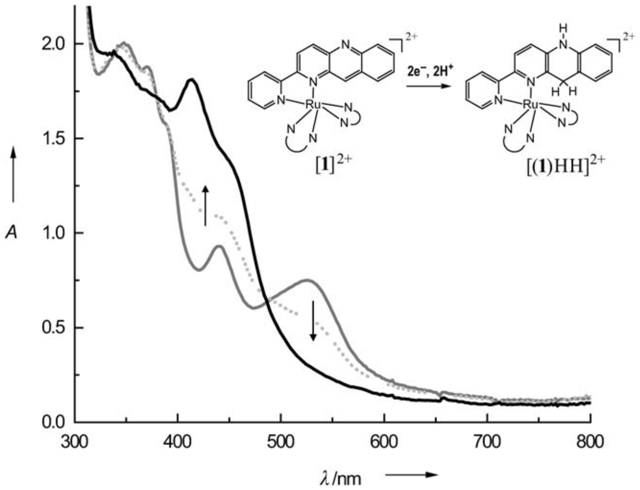

Figure 4. UV/Vis spectral change of $[\mathbf{1}]^{2+}$ to produce $[(\mathbf{1})HH]^{2+}$ in CH_3CN/Et_3N (4:1, v/v) upon irradiation at (355 ± 6) nm.

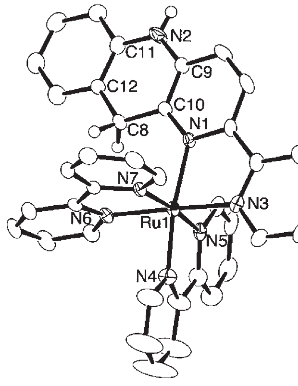

Figure 5. ORTEP drawing of the structure of $[(\mathbf{1})\text{HH}]^{2+}$ with 50-% thermal ellipsoids. Hydrogen atoms except H1 (attached to N2), H8, and H9 (attached to C8) are omitted for simplicity. Selected bond lengths [Å] and angles [°]: Ru–N1 2.131(3), Ru–N3 2.054(2), Ru–N4 2.041(3), Ru–N5 2.059(2), Ru–N6 2.077(2), Ru–N7 2.065(2), C8–C10 1.510(4), C8–C12 1.498(6), N2–C9 1.371(6), N2–C11 1.388(5); C10-C8-C12 114.7(3), C9-N2-C11 124.2(3).

compared with those of $[\mathbf{1}]^{2+}$ (1.376(10) and 1.399(9) Å) demonstrates the formation of the 1,4-dihydropyridine framework in the pbnHH ligand.

Exposure of Ar-degassed aqueous solutions containing $[\mathbf{1}]^{2+}$ and 10 mM NaHCO$_2$ to γ-ray irradiation (^{60}Co source) allowed production of $[(\mathbf{1})\text{HH}]^{2+}$ by strong reducing reagents (e^-_{aq} and $CO_2^{\bullet -}$) generated in situ. To understand the acid–base properties and the reactivity of the one-electron-reduced species of $[\mathbf{1}]^{2+}$, we prepared $[\mathbf{1}]^{+}$ using the reaction of $[\mathbf{1}]^{2+}$ with $CO_2^{\bullet -}$ generated by the pulse radiolysis technique as described previously.[5] Reduction of $[\mathbf{1}]^{2+}$ by $CO_2^{\bullet -}$ is first order in the concentration of $[\mathbf{1}]^{2+}$ and a rate constant of $5\times 10^9\,\text{M}^{-1}\,\text{s}^{-1}$ is measured between pH 3 and 11. The pH-dependent transient absorption spectra point toward formation of the one-electron-reduced species, $[\mathbf{1}]^{+}$, and its protonated analogue, $[\text{H}(\mathbf{1})]^{2+}$ (pK_a 11), consistent with the electrochemical results in Figure 2. Above pH 12, the transient spectra are similar to that obtained by Na–Hg reduction in CH$_3$CN. The protonation is fast and completes in our time resolution even at pH 10, which suggests the involvement of the phosphate buffer through hydrogen bonding. Between pH 3 and 13, a bimolecular decay of the transient species $[\text{H}(\mathbf{1})]^{2+}$ was observed as a major reaction pathway, which suggests that the species reacts via disproportionation to form $[\mathbf{1}]^{2+}$ and $[(\mathbf{1})\text{HH}]^{2+}$. Our preliminary results indicate the lack of a kinetic isotope effect for the disproportionation reaction. Detailed mechanistic and kinetic studies are under way and will be published separately.

In conclusion, $[(\mathbf{1})\text{HH}]^{2+}$ was produced cleanly by the photochemical reduction of $[\mathbf{1}]^{2+}$, which avoids the carbon-centered radical–radical coupling of $[\mathbf{1}]^{+}$ or $[\text{H}(\mathbf{1})]^{2+}$ radicals because of the steric interaction associated with the bulky {Ru(bpy)$_2$} moiety. This type of system would allow not only to investigate excited-state proton-coupled electron-transfer reactions with a number of quenchers that can provide protons, but also to explore potential catalytic hydride (or hydrogen-atom) transfer reactions from the hydrogenated product and/or the protonated one-electron-reduced species.

Experimental Section

Materials: [Ru(bpy)$_2$(pbn)](PF$_6$)$_2$ ([**1**](PF$_6$)$_2$) was prepared as previously described[3,6] and characterized by NMR, UV/Vis, and IR spectroscopy and ESI mass spectrometry. [Ru(bpy)$_2$(pbnHH)](PF$_6$)$_2$ ([(**1**)HH](PF$_6$)$_2$) was prepared in the following way: Addition of an aqueous solution of Na$_2$S$_2$O$_4$ (19 mg, 10.7 μmol in 5 mL) to a degassed acetonitrile solution of [**1**](PF$_6$)$_2$ (49 mg, 5.1 mmol in 20 mL) caused a rapid change of the color of the solution from red-brown to orange. After stirring the mixture for 2 h at room temperature, the solution was concentrated to ca. 1 mL by a rotary evaporator. Addition of an aqueous solution of NH$_4$PF$_6$ to the solution precipitated orange microcrystals, which were collected and dried in vacuo (38 mg, 78 % yield). HR-ESI MS: m/z 336.5725 $[M-2\,\text{PF}_6]^{2+}$. Photochemical reduction of [**1**](PF$_6$)$_2$ was conducted in either CH$_3$CN/Et$_3$N (4:1, v/v) under vacuum or N$_2$-bubbled DMF/TEOA (4:1, v/v). The solution was irradiated with either monochromatic light or light through a cutoff filter from a 75- or 150-W lamp.

DFT calculations: Gas- and solution-phase DFT calculations on $[\mathbf{1}]^{2+}$ were carried out with the hybrid B3LYP method and the Hay–Wadt VDZ ($n+1$) ECP (LANL2DZ ECP) 5d basis set. Geometry optimizations and frequency analyses were performed using the Gaussian 03 package of programs.[7]

Measurements: Spectroscopic measurements, flash photolysis, pulse radiolysis, and electrochemical measurements are presented in detail in the Supporting Information.

Received: January 22, 2007
Published online: April 20, 2007

Keywords: charge transfer · hydrides · NADH · photochemistry · ruthenium

---

[1] a) C. Walsh, *Acc. Chem. Res.* **1980**, *13*, 148, and references therein; b) D. M. Stout, A. I. Meyers, *Chem. Rev.* **1982**, *82*, 223.

[2] See, for example: a) S. Fukuzumi in *Advances in Electron-Transfer Chemistry* (Ed.: P. S. Mariano), JAI, Greenwich, CT, **1992**, pp. 67–175; b) J. Gębicki, A. Marcinek, J. Zielonka, *Acc. Chem. Res.* **2004**, *37*, 379; c) S. Fukuzumi, O. Inada, T. Suenobu, *J. Am. Chem. Soc.* **2003**, *125*, 4808; d) X.-Q. Zhu, Y. Yang, M. Zhang, J.-P. Cheng, *J. Am. Chem. Soc.* **2003**, *125*, 15298; e) I. Nakanishi, K. Ohkubo, S. Fujita, S. Fukuzumi, T. Konishi, M. Fujitsuka, O. Ito, N. Miyata, *J. Chem. Soc. Perkin Trans. 2* **2002**, 1829; f) S. Fukuzumi, H. Imahori, K. Okamoto, H. Yamada, M. Fujitsuka, O. Ito, D. M. Guldi, *J. Phys. Chem. A* **2002**, *106*, 1903; g) R. Reichenbach-Klinke, M. Kruppa, B. König, *J. Am. Chem. Soc.* **2002**, *124*, 12999; h) X.-Q. Zhu, H.-R. Li, Q. Li, T. Ai, J.-Y. Lu, Y. Yang, J.-P. Cheng, *Chem. Eur. J.* **2003**, *9*, 871; i) Y. Lu, Y. Zhao, K. L. Handoo, V. D. Parker, *Org. Biomol. Chem.* **2003**, *1*, 173; j) U. Gran, *Tetrahedron* **2003**, *59*, 4303; k) X.-Q. Zhu, L. Cao, Y. Liu, Y. Yang, J.-Y. Lu, J.-S. Wang, J.-P. Cheng, *Chem. Eur. J.* **2003**, *9*, 3937; l) Y. Mikata, S. Aida, S. Yano, *Org. Lett.* **2004**, *6*, 2921; m) C. Selvaraju, P. Ramamurthy, *Chem. Eur. J.* **2004**, *10*, 2253; n) S. C. Ritter, M. Eiblmaier, V. Michlova, B. König, *Tetrahedron* **2005**, *61*, 5241; o) H. Buck, *Int. J. Quantum Chem.* **2005**, *101*, 389; p) O. Ishitani, N. Inoue, K. Koije, T. Ibusuki, *J. Chem. Soc. Chem. Commun.* **1994**, 367; q) A. Kobayashi, K. Sakamoto, O. Ishitani, *Inorg. Chem. Commun.* **2005**, *8*, 365; r) A. Kobayashi, H. Konno, K. Sakamoto, A. Sekine, Y. Ohashi, M. Iida, O. Ishitani, *Chem. Eur. J.* **2005**, *11*, 4219; s) M. Tanaka, K. Ohkubo, S. Fukuzumi, *J. Am. Chem. Soc.* **2006**, *128*, 12372; t) J. Yuasa, S. Fukuzumi, *J. Am. Chem. Soc.* **2006**, *128*, 14281; u) J. Yuasa, S. Yamada, S. Fukuzumi, *J. Am. Chem. Soc.* **2006**, *128*, 14938, and references therein.

[3] T. Koizumi, K. Tanaka, *Angew. Chem.* **2005**, *117*, 6041; *Angew. Chem. Int. Ed.* **2005**, *44*, 5891.

[4] Crystallographic data for ([**1**]HH)$(PF_6)_2 \cdot 2\,CH_3CN$: monoclinic, $P\bar{1}$ (no. 2), $a = 9.442(3)$, $b = 14.306(5)$, $c = 17.633(5)$ Å, $\alpha = 74.14(2)$, $\beta = 74.30(1)$, $\gamma = 72.41(1)°$, $V = 2138(1)$ Å^3, $Z = 2$, $\rho_{calcd} = 1.623\ g\,cm^{-3}$, $\mu(Mo_{K\alpha}) = 5.378\ cm^{-1}$, $R1 = 0.070$ ($I > 2\sigma(I)$), and $wR = 0.164$ for 9376 unique data reflections and 588 parameters. A red block crystal with approximate dimensions of $0.20 \times 0.10 \times 0.10$ mm was mounted in a loop. Data were collected at −160°C on a Rigaku/MSC Mercury CCD diffractometer by using graphite-monochromated $Mo_{K\alpha}$ radiation (0.71070 Å). All data were collected and processed using the Crystal Clear program (Rigaku). Calculations were performed using the CrystalStructure crystallographic software package. All structures were solved by direct methods and expanded using Fourier techniques. Refinements were performed anisotropically for all non-hydrogen atoms except acetonitrile molecules and disordered atoms by the full-matrix least-squares method. Hydrogen atoms for $[(\mathbf{1})HH]^{2+}$ were placed at the calculated positions and were included in the structure calculation without further refinement of the parameters, except the hydrogen atoms attached to C8 and N2. One PF_6^- anion is disordered into two positions. Detailed results can be found in the Supporting Information. CCDC-633445 contains the supplementary crystallographic data for this paper. These data can be obtained free of charge from The Cambridge Crystallographic Data Centre via www.ccdc.cam.ac.uk/data_request/cif.

[5] a) M. D'Angelantonio, Q. G. Mulazzani, M. Ventura, M. Ciano, M. Z. Hoffman, *J. Chem. Phys.* **1991**, *95*, 5121; b) H. Sun, M. Z. Hoffman, *J. Phys. Chem.* **1993**, *97*, 5014; c) F. Casalboni, Q. G. Mulazzani, C. D. Clark, M. Z. Hoffman, P. L. Orizondo, M. W. Perkovic, D. P. Rillema, *Inorg. Chem.* **1997**, *36*, 2252; d) F. Casalboni, Q. G. Mulazzani, R. L. Cleary, M. D. Ward, *J. Chem. Phys. A* **1998**, *102*, 5749.

[6] a) A. Godard, G. Quéguiner, *J. Heterocycl. Chem.* **1980**, *17*, 465; b) A. Godard, G. Quéguiner, *J. Heterocycl. Chem.* **1982**, *19*, 1289.

[7] Gaussian 03 (Revision C.02) M. J. Frisch et al., see the Supporting Information.